Sensitivity of angle-resolved photoemission to short-range antiferromagnetic correlations

R. Wallauer,[1] S. Sanna,[2] E. Lahoud,[1] P. Carretta,[2] and A. Kanigel[1]
[1]*Technion - Israel Institute of Technology, Department of Physics, Technion City, 32000 Haifa, Israel*
[2]*Dipartimento di Fisica and Unit CNISM di Pavia, I-27100 Pavia, Italy*
(Received 20 October 2014; published 24 June 2015)

Angle-resolved photoemission spectroscopy (ARPES) is one of most powerful techniques to unravel the electronic properties of layered materials and, in recent decades, it has lead to significant progress in the understanding of the band structures of cuprates, pnictides, and other materials of current interest. On the other hand, its application to Mott-Hubbard insulating materials where a Fermi surface is absent has been more limited. Here we show that in these latter materials, where electron spins are localized, ARPES may provide significant information on the spin correlations which can be complementary to the one derived from neutron-scattering experiments. $Sr_2Cu_{1-x}Zn_xO_2Cl_2$, a prototype of a diluted spin $S = 1/2$ antiferromagnet (AF) on a square lattice, was chosen as a test case and a direct correspondence between the amplitude of the spectral weight beyond the AF zone boundary derived from ARPES and the spin-correlation length ξ estimated from ^{35}Cl NMR was established. It was found that even for correlation lengths of a few lattice constants, a significant spectral weight in the backbended band is present which depends markedly on ξ. Moreover, the temperature dependence of that spectral weight is found to scale with the x-dependent spin stiffness. These findings prove that the ARPES technique is very sensitive to short-range correlations and its relevance in the understanding of the electronic correlations in cuprates is discussed.

DOI: 10.1103/PhysRevB.91.245149 PACS number(s): 74.72.Cj, 74.25.Jb, 75.25.−j, 79.60.−i

The discovery of high-temperature superconductivity in the cuprates has promoted a renewed interest in the study of electron-spin correlations in quantum $S = 1/2$ spin systems. Inelastic neutron-scattering (INS) [1] and nuclear spin-lattice relaxation rate $(1/T_1)$ [2] measurements have been widely employed to investigate the evolution of spin correlation in several layered materials such as cuprates, manganites, and pnictides [3] and a series of major breakthroughs have been obtained. Nevertheless, each one of these techniques has its drawbacks. Inelastic neutron scattering requires large crystals which are not always available, while the determination of the spin-correlation length ξ from nuclear magnetic resonance (NMR) $1/T_1$ is not direct but rather based on scaling assumptions. Only when scaling exponents are known, as is the case for the cuprates, does NMR $1/T_1$ allow a quantitative estimate of ξ [4].

Remarkably, the onset of sizable antiferromagnetic (AF) correlations can also affect the band structure. In fact, due to the AF order, the Brillouin-zone boundary is reduced to half of its size in the ordered state and electron bands bend back at the AF zone boundary. Hence, it is tempting to use a technique which is quite sensitive to the details of the band features, as it is in the case of angle-resolved photoemission spectroscopy (ARPES), to investigate the electron-spin correlations. ARPES has provided clarification as to how the Fermi surface of high-T_c superconductors (HTSC) evolves with hole doping and which parts are likely involved in the pairing mechanisms [5], becoming one of the most attractive techniques to study electronic correlations in layered materials. On the other hand, the charge density wave (CDW) instabilities recently detected in HTSC [6–8] are somewhat elusive to ARPES since often they do not give rise to the typical "fingerprints" of CDW order [9,10]. For example, the change in the Fermi momentum observed in Bi2201 [11], which could result from a CDW phase, is not observed in Bi2212 [12]. Accordingly, it has been argued that the absence of a signature of CDW order in ARPES spectra could likely be due to the short-range or even dynamic character of the CDWs. Here we show that, on the contrary, ARPES is sensitive to short-range electron-spin correlations and may represent a sensitive probe, complementary to INS, particularly when the correlation length approaches a few lattice steps.

We have chosen $Sr_2CuO_2Cl_2$ (SCOC), one of the best experimental realizations of a spin $S = 1/2$ two-dimensional (2D) antiferromagnet on a square lattice, as a test case for ARPES sensitivity to short-range spin correlations. This material is characterized by a well-defined order parameter and magnetic wave vector $\vec{q}$. Moreover, its in-plane AF correlation length ξ above the Néel temperature T_N was studied using INS [13,14], resonant inelastic x-ray scattering (RIXS) [15], and ^{35}Cl NMR [16]. In addition, due to the presence of a natural cleaving plane, SCOC is perfectly suited for ARPES experiments.

Many ARPES studies have been carried out on SCOC [17–22] and on the nearly identical $Ca_2CuO_2Cl_2$ system [23,24], both below and above T_N. As expected, owing to the AF ordering, the Brillouin-zone boundary is reduced to half of its size in the ordered state and the band bends back at the antiferromagnetic zone boundary (see inset in Fig. 1). Remarkably, even if this backbending is believed to be a result of the AF order, it persists up to temperatures well above $T_N = 256$ K. This can be explained by the very long AF correlations which are about 100 lattice constants at 300 K [13]. In this work, we were able to reduce ξ down to a few lattice constants a, measure with ARPES the intensity in the backbended part, and relate it to a change in the correlation length estimated from ^{35}Cl NMR $1/T_1$ measurements. As will be shown in the following, some intensity in the backbended part persists even for $\xi/a \simeq 3$. This represents a systematic study of the sensitivity of ARPES to the AF correlation length,

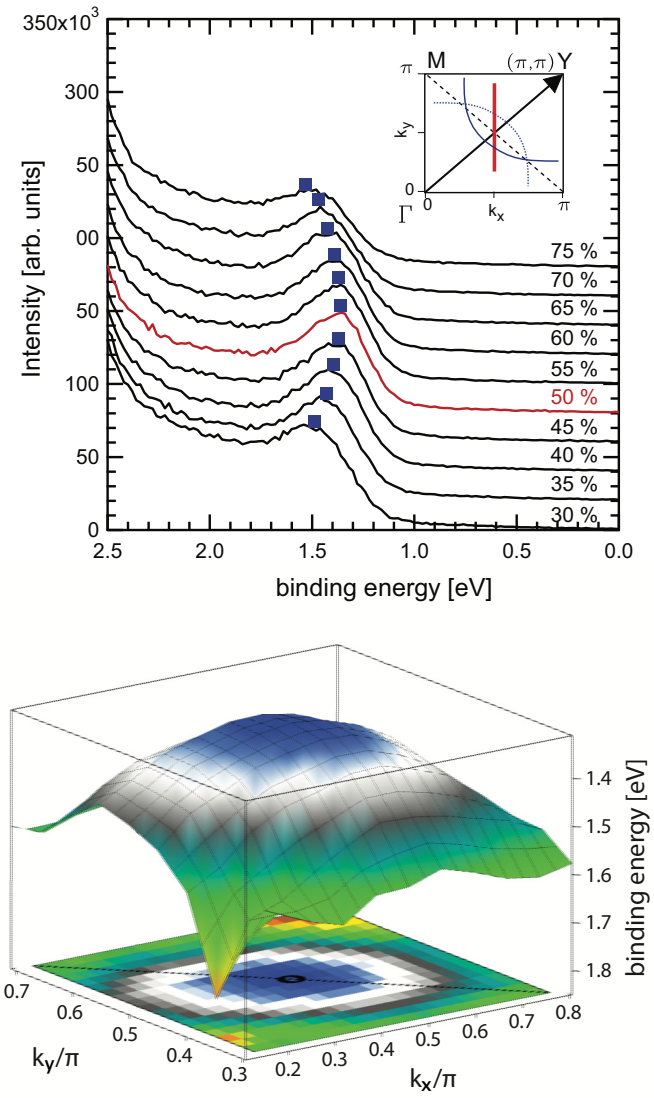

FIG. 1. (Color online) Upper panel: Band dispersion along the Γ-*M* direction around the $(\pi/2,\pi/2)$ point. The position of the peak in each EDC is indicated by blue dots and we find the lowest binding energy at the AFM zone boundary (red line). Inset: A typical cuprate Fermi surface and the folded band upon antiferromagnetic ordering with wave vector $\vec{q} = (\pi,\pi)$ (black arrow). Lower panel: Extracted dispersion from peak position of several scans in the Γ-*M* direction. The top of the band moves from the zone corner to $(\pi/2,\pi/2)$, as indicated by the black circle in the 2D projection.

which can be relevant also for the understanding of other fluctuating orders.

SCOC single crystals were grown from the melt according to the procedure described by Miller *et al.* [25]. All ARPES measurements were done with 21.2 eV photons from a monochromized He lamp and a Scienta R4000 electron analyzer. Due to the broad band under investigation and for the sake of better statistics, spectra were typically recorded with 20 meV energy resolution and 0.2 degree angular resolution. Figure 1 shows the dispersion of the highest occupied band at 300 K in the direction indicated by the red line in the inset. A minimal binding energy of about 1.4 eV is found exactly at the AF zone boundary, indicated by the red curve. Beyond that point, the band bends back toward higher binding energies, as expected in view of the new periodicity of the system. At high binding energies around the zone center, we find a waterfall-like feature, typical of many cuprates, whose origin is still under debate [26–28]. We note that since SCOC is insulating, the chemical potential is set by impurity levels and can vary significantly between different samples. For that reason, the gap size cannot be measured.

In agreement with previous works, we find no sharp peaks even at the lowest binding energy. The origin of the line broadening still needs to be clarified since numerical calculations based on the *t*-*J* model actually predict sharp quasiparticlelike excitations [19,29–33]. By measuring several momentum cuts and extracting the peak positions for each energy distribution curve (EDC), we were able to map the dispersion of the band over a large area of the Brillouin zone (see Fig. 1, lower panel). The dispersion is symmetric around the new zone boundary and has a maximum at $(\pi/2,\pi/2)$. We repeated the measurements at various temperatures between 77 K, deep in the AF-ordered phase, and up to 450 K, nearly twice T_N. We find almost no change in the spectra and, in particular, at all temperatures we observe the backbended band beyond $(\pi/2,\pi/2)$. However, it should be noticed that in SCOC even at 450 K, $k_B T \ll J$, the in-plane superexchange coupling, and the correlation length is still more than 20 lattice constants [13].

In order to reduce the correlation length, we partially substituted $S = 1/2$-Cu^{2+} ions by spinless Zn^{2+} ions. In fact, it is well established that in $La_2Cu_{1-x}(Zn,Mg)_xO_4$, T_N can be reduced by diluting the spin lattice [4,34,35], and long-range order can even be completely suppressed for substitution levels beyond the percolation threshold (41% for a square lattice). More important for our needs, Zn can significantly reduce the AF correlation length ξ above T_N. We found that Zn can substitute Cu in SCOC crystals up to the substitution limit of 29%, a value below the percolation threshold but large enough to yield a significant reduction of the AF correlations and of T_N. In particular, at this substitution level, T_N is reduced to 180 K.

The ARPES spectra of the the spin-diluted samples, at all temperatures and at all Zn concentrations, still show intensity beyond the AF zone boundary. In particular, in Fig. 2, we show two normalized ARPES images for the $x = 0.29$ sample, in which each spectrum is normalized using the intensity at high-binding energy around the Γ point, and a constant background, measured at low binding energy in the Mott gap, was subtracted. In the left panel of Fig. 2, we show an image measured at $T = 77$ K in the AF state and, on the right, the corresponding image at $T = 400$ K, where the correlation length is only three lattice constants based on the high-temperature extrapolation of the NMR data. One can clearly see that even if at 400 K the intensity of the backbended part is much weaker than at 77 K, there is still some intensity beyond the AF zone boundary.

In order to provide a quantitative estimate of that intensity, we performed the following analysis. We integrate the intensity along the dispersion maximum on both sides of the $(\pi/2,\pi/2)$ point (dashed white line in Fig. 2), as indicated by the black (*A*) and red (*B*) lines. The range of the integration area is 300 meV along the energy axis. Along the momentum axis,

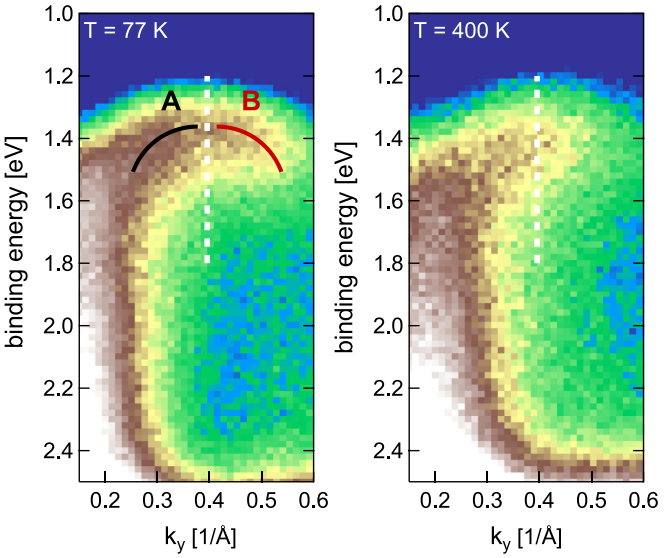

FIG. 2. (Color online) Comparison of the ARPES images for the $x = 0.29$ substituted sample at 77 (left) and 400 (right) K. The loss of spectral weight beyond the $(\pi/2,\pi/2)$ point, indicated by the white line, can be observed at high temperature. Nevertheless, the backbended band is clearly visible, although the correlation length at this temperature is 2–3 lattice constants. The black (A) and red (B) lines represent the band dispersion on both sides of the new zone boundary at $(\pi/2,\pi/2)$.

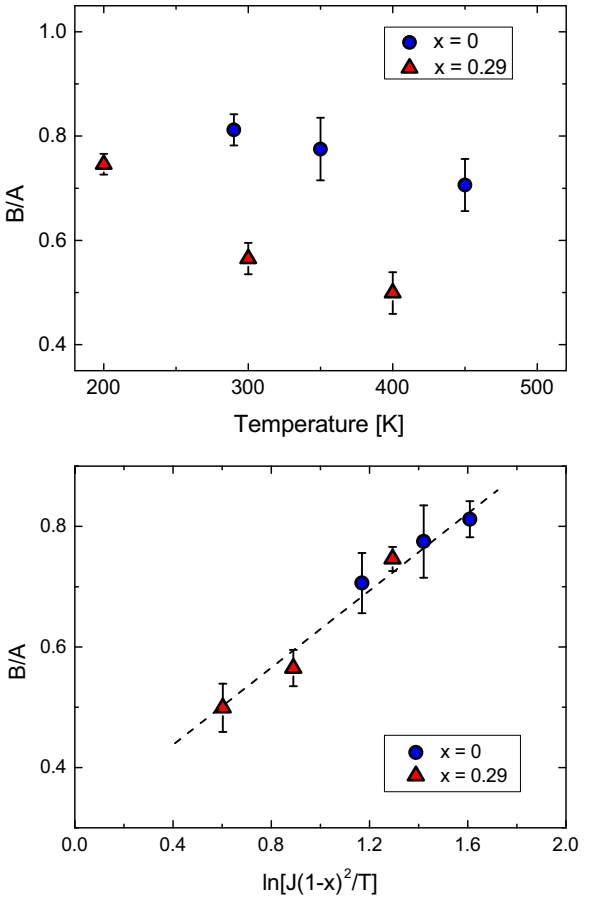

FIG. 3. (Color online) (a) The ratio of the integrated intensity along the black (A) and red (B) lines in Fig. 2 as a function of the temperature. (b) The ratio B/A is reported as a function of $\ln[J(1-x)^2/T]$ in order to evidence the scaling of its T dependence with the spin stiffness.

we choose a range that starts at a point near the Γ point, where the dispersion is not affected by the waterfall-like feature, and ends at the $(\pi/2,\pi/2)$ point. An identical range was chosen on the other side of the $(\pi/2,\pi/2)$ point. Thus, the ratio of the integrals on both sides, B/A, provides a measure of the loss of spectral weight beyond the AF zone boundary.

In Fig. 3(a), we show the ratio B/A as a function of temperature for the pristine and for the $x = 0.29$ samples. For the pristine sample, the ratio B/A decreases rather slowly with temperature, which is not surprising if one considers that this 2D AF is characterized by a $J \simeq 1450$ K. On the other hand, in the Zn-substituted sample, this ratio decreases faster with temperature. In a spin-diluted $S = 1/2$ Heisenberg AF on a square lattice, the T dependence of the in-plane correlation length $\xi \propto \exp[2\pi\rho_s(x)/T]$ is determined by the spin stiffness $\rho_s(x) = 1.15J(1-x)^2/2\pi$ [4,34], where the factor $(1-x)^2$ accounts for the probability to find two neighboring electron spins coupled via the exchange coupling J. Accordingly, one should expect that if the B/A ratio is a measure of the spin correlations, it should scale as $J(1-x)^2/T$. Remarkably, in Fig. 3(b), one observes that such a scaling does occur and that $B/A \propto \ln[J(1-x)^2/T]$. The understanding of this logarithmic functional form goes beyond the aim of the present work.

In order to further evidence the direct relationship between the B/A ratio and the in-plane correlation length, we quantitatively estimated ξ for different spin-diluted samples. ξ can be conveniently derived from the nuclear spin-lattice relaxation rate $1/T_1$, an approach successfully used in the analogous $La_2Cu_{1-x}Zn_xO_4$ compound [4] where a quantitative agreement with the ξ directly measured by INS was found. In fact, by resorting to scaling arguments, once the hyperfine coupling A and dynamical scaling exponent z are known, one can establish a one-to-one correspondence between $1/T_1$ and ξ [4]. In particular, if one considers a 2D $S = 1/2$ antiferromagnet on a square lattice and a nucleus which is essentially coupled just with its nearest neighbor $S = 1/2$ spin, one can write

$$\frac{1}{T_1} = \frac{\gamma^2 A^2}{4}\frac{\hbar\sqrt{\pi}}{Jk_B}\xi^{z+2}\beta(\xi)\int_{BZ}\frac{d\vec{q}}{(1+q^2\xi^2)^2}, \qquad (1)$$

with γ the nuclear gyromagnetic ratio and $1/\beta(\xi) = \xi^2\int_{BZ} d\vec{q}/(1+q^2\xi^2)$ a factor which preserves the spin sum rule [4]. For $\xi \gg 1$, this expression yields to $1/T_1 \propto \xi^z$. In SCOC, one can assume the dynamical scaling exponent $z = 1$ derived from INS [13] and nuclear quadrupole resonance (NQR) experiments [4] for other cuprates on a square lattice, such as La_2CuO_4. Since A was not very precisely estimated from previous shift measurements [16], we decided to determine it by taking for A the value which allows one to match the absolute value for ξ determined from ^{35}Cl $1/T_1$ and from INS over the same T range. Such a match occurs for $A \simeq 2.7$ kOe, which is a value very close to the one that can be derived from the high-T limit of $1/T_1$. In the case of diluted samples, one

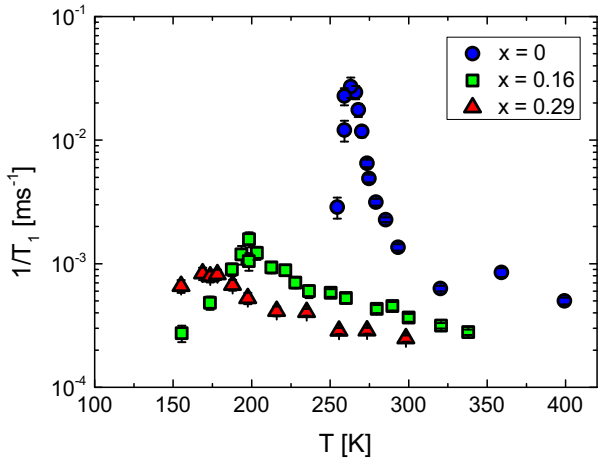

FIG. 4. (Color online) Temperature dependence of ^{35}Cl $1/T_1$ in $Sr_2Cu_{1-x}Zn_xO_2Cl_2$ for $x = 0, 0.16, 0.29$ measured in a 5.6 Tesla magnetic field. T_N is reduced by the Zn substitution, as can be measured by following the peak position in $1/T_1$ as the Zn concentration is increased.

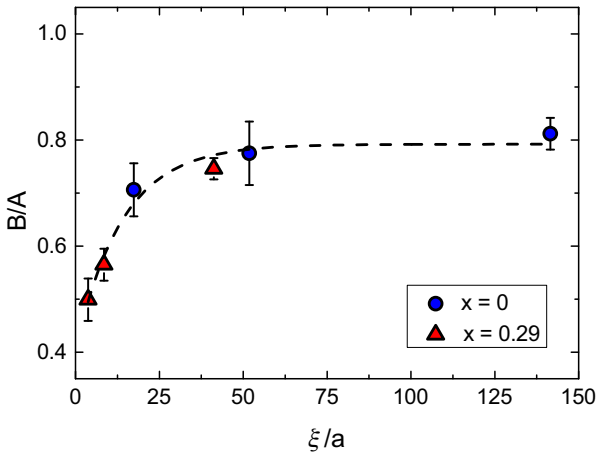

FIG. 6. (Color online) The ratio B/A is reported as a function of correlation length as measured by NMR data (see Fig. 5). The dashed line is a guide to the eye.

has to consider a correction of the average hyperfine coupling by a factor $(1-x)$ [4], accounting for the probability that ^{35}Cl nuclear spin is coupled to the nearest-neighbor Cu^{2+} spin.

The temperature dependence of ^{35}Cl $1/T_1$, determined by using standard radio-frequency pulse sequences, is shown in Fig. 4 for three representative samples. One observes that $1/T_1$ progressively increases upon cooling, shows a peak at T_N, and decreases upon further cooling. The progressive growth of $1/T_1$ upon approaching T_N from above is associated with the progressive growth of the in-plane AF correlations [see Eq. (1)] [16]. One can now use Eq. (1) to derive $\xi(T,x)$ from $1/T_1$ data. The temperature dependence of $\xi(x,T)$ is shown in Fig. 5. One notices that for the diluted samples, the correlation length grows exponentially on decreasing temperature, while for the undoped SCOC, a crossover to an XY behavior, characterized by a more rapid increase of ξ, is observed on approaching T_N, as pointed out by previous NMR experiments [16].

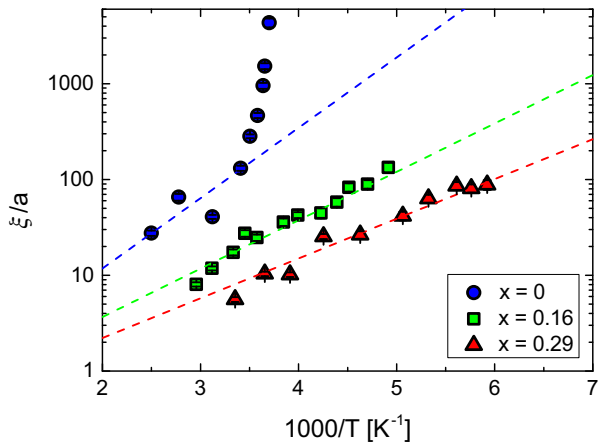

FIG. 5. (Color online) The AF correlation length in units of lattice constants as a function of $1/T$ for three different Zn concentrations. ξ was calculated from the $1/T_1$ data using Eq. (1). The dashed lines show the exponential growth expected for a two-dimensional $S = 1/2$ antiferromagnet. The deviation from that trend observed for $x = 0$ at $T \to T_N$ was ascribed to a small planar spin anisotropy [16].

In Fig. 6, we show the dependence of the ARPES intensity B/A ratio on the correlation length determined from ^{35}Cl $1/T_1$. We find that for both samples, the intensity beyond the AF zone boundary as measured by ARPES is controlled by the AF correlation length. For $\xi \leqslant 15$ lattice units, the B/A ratio shows a significant dependence on ξ, which clearly demonstrates that ARPES spectra are indeed sensitive to AF correlations even when they are as short as a few lattice constants. This is evidence that ARPES, besides being a well-established technique to investigate the electronic structure of layered materials, allows one to also detect short-range electron-spin correlations. For correlation lengths larger than 15 lattice constants, we observe almost no change in the spectra and hence it is not possible to distinguish the AF long-range order from a fluctuating phase characterized by ξ of the order of tens of lattice constants.

In conclusion, we have shown that the backbended part of the highest occupied band changes upon decreasing correlation length. This can be seen as a proof that AF correlations are indeed responsible for this backbending and that ARPES is a sensitive probe to very short-range AF correlations. Using Zn substitution and by suitably increasing the temperature, we were able to control the correlation length down to three constants verified by NMR measurements. Even for the shortest correlation length, the spectra surprisingly showed significant spectral weight beyond the AF zone boundary.

The ARPES ability to detect short-range correlations has relevant implications also for other kinds of order. In particular, our findings suggest that the absence of the expected fingerprints of a CDW instability in the ARPES spectra of the underdoped cuprates is not simply a consequence of the short range of the CDW correlations.

R.W. acknowledges support by the BMBF through the Minerva Fellowship program.

[1] B. Keimer, N. Belk, R. J. Birgeneau, A. Cassanho, C. Y. Chen, M. Greven, M. A. Kastner, A. Aharony, Y. Endoh, R. W. Erwin, and G. Shirane, Phys. Rev. B **46**, 14034 (1992).

[2] A. Rigamonti, F. Borsa, and P. Carretta, Rep. Prog. Phys. **61**, 1367 (1998).

[3] G. S. Tucker, D. K. Pratt, M. G. Kim, S. Ran, A. Thaler, G. E. Granroth, K. Marty, W. Tian, J. L. Zarestky, M. D. Lumsden, S. L. Bud'ko, P. C. Canfield, A. Kreyssig, A. I. Goldman, and R. J. McQueeney, Phys. Rev. B **86**, 020503 (2012).

[4] P. Carretta, A. Rigamonti, and R. Sala, Phys. Rev. B **55**, 3734 (1997).

[5] A. Damascelli, Rev. Mod. Phys. **75**, 473 (2003).

[6] T. Wu, H. Mayaffre, S. Kramer, M. Horvatic, C. Berthier, W. N. Hardy, R. Liang, D. A. Bonn, and M.-H. Julien, Nature (London) **477**, 191 (2011).

[7] G. Ghiringhelli, M. Le Tacon, M. Minola, S. Blanco-Canosa, C. Mazzoli, N. B. Brookes, G. M. De Luca, A. Frano, D. G. Hawthorn, F. He, T. Loew, M. M. Sala, D. C. Peets, M. Salluzzo, E. Schierle, R. Sutarto, G. A. Sawatzky, E. Weschke, B. Keimer, and L. Braicovich, Science **337**, 821 (2012).

[8] J. Chang, E. Blackburn, A. T. Holmes, N. B. Christensen, J. Larsen, J. Mesot, R. Liang, D. A. Bonn, W. N. Hardy, A. Watenphul, M. v. Zimmermann, E. M. Forgan, and S. M. Hayden, Nat. Phys. **8**, 871 (2012).

[9] V. Brouet, W. L. Yang, X. J. Zhou, Z. Hussain, N. Ru, K. Y. Shin, I. R. Fisher, and Z. X. Shen, Phys. Rev. Lett. **93**, 126405 (2004).

[10] E. Lahoud, O. N. Meetei, K. B. Chaska, A. Kanigel, and N. Trivedi, Phys. Rev. Lett. **112**, 206402 (2014).

[11] M. Hashimoto, Nat. Phys. **6**, 414 (2010).

[12] A. Kanigel, U. Chatterjee, M. Randeria, M. R. Norman, G. Koren, K. Kadowaki, and J. C. Campuzano, Phys. Rev. Lett. **101**, 137002 (2008).

[13] M. Greven, R. J. Birgeneau, Y. Endoh, M. A. Kastner, B. Keimer, M. Matsuda, G. Shirane, and T. R. Thurston, Phys. Rev. Lett. **72**, 1096 (1994).

[14] K. W. Plumb, A. T. Savici, G. E. Granroth, F. C. Chou, and Y.-J. Kim, Phys. Rev. B **89**, 180410 (2014).

[15] M. Guarise, B. Dalla Piazza, M. Moretti Sala, G. Ghiringhelli, L. Braicovich, H. Berger, J. N. Hancock, D. van der Marel, T. Schmitt, V. N. Strocov, L. J. P. Ament, J. van den Brink, P.-H. Lin, P. Xu, H. M. Rønnow, and M. Grioni, Phys. Rev. Lett. **105**, 157006 (2010).

[16] F. Borsa, M. Corti, T. Goto, A. Rigamonti, D. C. Johnston, and F. C. Chou, Phys. Rev. B **45**, 5756 (1992).

[17] B. O. Wells, Z. X. Shen, A. Matsuura, D. M. King, M. A. Kastner, M. Greven, and R. J. Birgeneau, Phys. Rev. Lett. **74**, 964 (1995).

[18] S. LaRosa, I. Vobornik, F. Zwick, H. Berger, M. Grioni, G. Margaritondo, R. J. Kelley, M. Onellion, and A. Chubukov, Phys. Rev. B **56**, R525 (1997).

[19] J. J. M. Pothuizen, R. Eder, N. T. Hien, M. Matoba, A. A. Menovsky, and G. A. Sawatzky, Phys. Rev. Lett. **78**, 717 (1997).

[20] C. Dürr, S. Legner, R. Hayn, S. V. Borisenko, Z. Hu, A. Theresiak, M. Knupfer, M. S. Golden, J. Fink, F. Ronning, Z.-X. Shen, H. Eisaki, S. Uchida, C. Janowitz, R. Müller, R. L. Johnson, K. Rossnagel, L. Kipp, and G. Reichardt, Phys. Rev. B **63**, 014505 (2000).

[21] S. Haffner, C. G. Olson, L. L. Miller, and D. W. Lynch, Phys. Rev. B **61**, 14378 (2000).

[22] S. Haffner, D. M. Brammeier, C. G. Olson, L. L. Miller, and D. W. Lynch, Phys. Rev. B **63**, 212501 (2001).

[23] F. Ronning, C. Kim, D. L. Feng, D. S. Marshall, A. G. Loeser, L. L. Miller, J. N. Eckstein, I. Bozovic, and Z.-X. Shen, Science **282**, 2067 (1998).

[24] F. Ronning, K. M. Shen, N. P. Armitage, A. Damascelli, D. H. Lu, Z.-X. Shen, L. L. Miller, and C. Kim, Phys. Rev. B **71**, 094518 (2005).

[25] L. L. Miller, X. L. Wang, S. X. Wang, C. Stassis, D. C. Johnston, J. Faber, and C.-K. Loong, Phys. Rev. B **41**, 1921 (1990).

[26] D. S. Inosov, J. Fink, A. A. Kordyuk, S. V. Borisenko, V. B. Zabolotnyy, R. Schuster, M. Knupfer, B. Büchner, R. Follath, H. A. Dürr, W. Eberhardt, V. Hinkov, B. Keimer, and H. Berger, Phys. Rev. Lett. **99**, 237002 (2007).

[27] S. Basak, T. Das, H. Lin, J. Nieminen, M. Lindroos, R. S. Markiewicz, and A. Bansil, Phys. Rev. B **80**, 214520 (2009).

[28] J. Graf, G.-H. Gweon, K. McElroy, S. Y. Zhou, C. Jozwiak, E. Rotenberg, A. Bill, T. Sasagawa, H. Eisaki, S. Uchida, H. Takagi, D.-H. Lee, and A. Lanzara, Phys. Rev. Lett. **98**, 067004 (2007).

[29] C. Kim, F. Ronning, A. Damascelli, D. L. Feng, Z.-X. Shen, B. O. Wells, Y. J. Kim, R. J. Birgeneau, M. A. Kastner, L. L. Miller, H. Eisaki, and S. Uchida, Phys. Rev. B **65**, 174516 (2002).

[30] R. B. Laughlin, Phys. Rev. Lett. **79**, 1726 (1997).

[31] K. M. Shen, F. Ronning, D. H. Lu, W. S. Lee, N. J. C. Ingle, W. Meevasana, F. Baumberger, A. Damascelli, N. P. Armitage, L. L. Miller, Y. Kohsaka, M. Azuma, M. Takano, H. Takagi, and Z.-X. Shen, Phys. Rev. Lett. **93**, 267002 (2004).

[32] G. Sangiovanni, O. Gunnarsson, E. Koch, C. Castellani, and M. Capone, Phys. Rev. Lett. **97**, 046404 (2006).

[33] A. S. Mishchenko and N. Nagaosa, Phys. Rev. Lett. **93**, 036402 (2004).

[34] O. P. Vajk, P. K. Mang, M. Greven, P. M. Gehring, and J. W. Lynn, Science **295**, 1691 (2002).

[35] P. Carretta, G. Prando, S. Sanna, R. De Renzi, C. Decorse, and P. Berthet, Phys. Rev. B **83**, 180411(R) (2011).